Deviations from Liquidlike Behavior in Molten Polymer Films at Interfaces

Young-Soo Seo,[1] T. Koga,[1] J. Sokolov,[1] M. H. Rafailovich,[1] M. Tolan,[2] and S. Sinha[3]

[1]*Department of Material Science & Engineering, State University of New York at Stony Brook, New York 11794, USA*
[2]*Universitaet Dortmund, Experimentelle Physik I, Otto-Hahn-Strasse 4, D-44221 Dortmund, Germany*
[3]*Department of Physics, University of California, San Diego, 9500 Gilman Drive, La Jolla, California 92093, USA*

(Received 24 June 2004; published 22 April 2005)

We have performed x-ray specular and diffuse scattering on liquid polymer films and analyzed the spectra as a function of film thickness and molecular weight. The results show that films whose molecular weight is close to the entanglement length behave as simple liquids except that the shortest wavelength is determined by the radius of gyration (R_g) rather than the monomer-monomer distance. When the molecular weight is higher than the entanglement length, the strong deviations from liquidlike behavior are observed. We find that the long wavelength cutoff vector, $q_{l,c}$, scales with film thickness, d as $d^{-1.1\pm0.1}$ rather than the usual d^{-2} expected for simple liquids. If we assume that these deviations are due to surface pinning of the polymer chains, then our results are consistent with the formalism developed by Fredrickson *et al.* to explain the capillary wave spectrum that can propagate in a polymer brush.

DOI: 10.1103/PhysRevLett.94.157802 PACS numbers: 61.41.+e, 82.35.Lr, 83.80.Sg

Numerous groups have demonstrated that when polymer films are spun cast onto silicon substrates they are in a strongly confined state due to interactions with the Si surface [1–7]. Russell *et al.* [8] and subsequently others [9] have shown that these interactions can decrease the center of mass diffusion coefficient of polymer chains adjacent to the interface. Tolan *et al.* [10] have shown that these interactions can also affect the dispersion relation of the surface capillary waves and introduce an anomalous cutoff wave vector and effective Hamaker constant that was much larger than the usual one associated with the van der Waals interactions. A similarly large constant was also necessary to explain the attenuation of surface roughness of liquid polymer films on corrugated surfaces [11]. In all these cases, the authors demonstrated that these effects were not restricted to chains in direct contact with the interface, but persisted for distances significantly larger than the radius of gyration of the polymer chains, $R_g = a(N/6)^{1/2}$, with monomer size, a, and degree of polymerization, N.

In this Letter we explore the nature of the capillary wave spectra as a function of polymer molecular weight and film thickness. In this manner we are able to extract information regarding the effects of entanglements and internal polymer structure on the viscoelastic properties of thin polymer films and thereby obtain a fundamental understanding of the limitation of the simple liquid theory when applied to complex viscoelastic fluids.

An expression for the surface roughness due to capillary waves, σ, was derived by several groups from the capillary wave scattering structure factor [12]. They obtained

$$\sigma^2(d) = \sigma_{\text{in}}^2 + \frac{1}{2}B\ln\left[\frac{q_{u,c}}{q_{\text{vdW}}(d)}\right], \tag{1}$$

where σ_{in} is the intrinsic roughness on the order of molecular dimension, $q_{u,c} = 2\pi/\kappa \sim 0.1$–$1$ Å^{-1} is the upper wave vector cutoff, and κ is the size of a polymer molecule in the melt. $B = k_BT/(\pi\gamma)$ where k_B and T are the Boltzmann constant and absolute temperature, and γ is the surface tension of the film. The van der Waals' cutoff wave vector for simple liquids, q_{vdW}, is expressed by

$$q_{\text{vdW}}(d) = (A_{\text{eff}}/2\pi\gamma)^{1/2}/d^2, \tag{2}$$

where A_{eff} is an effective Hamaker constant. Subsequent experiments showed that this expression was most applicable to surfaces of low molecular weight liquids, where Tidswell *et al.* obtained the classical value $A_{\text{eff}} = 5.9 \times 10^{-20}$ J. In the case of viscoelastic complex fluids, Shin *et al.* [13] showed that Eq. (1) could only be used to fit the surfaces of free standing films where the gravitational cutoff becomes the dominant term instead of q_{vdW} since $A_{\text{eff}} = 0$ and $q_{u,c} = 1/a$ where $a = 6.7$ Å for polystyrene (PS). This indicates that in an unconfined polymer liquid the monomer-monomer distance rather than entanglements dominate the scattered x-ray intensity.

In the case of supported films, pinning of polymer chains by the surface introduces additional confinement and κ may no longer be simply the monomer-monomer distance. Li *et al.* [14] found that the capillary wave spectra of PS films supported on Si substrates could be fit with an equation having the same mathematical form as Eq. (1), except that the value of $A_{\text{eff}} \sim 10^{-17}$ J was unphysically large. Hence Eq. (1) became an indirect gauge of the adsorption strength of the polymer to the substrate, rather than a description of the capillary spectra.

In this Letter, we measure the capillary spectra at the surface of thin polymer films and show that the wave vector dependence becomes a function of the polymerization index. Namely, for $N \approx N_e$, where N_e is entanglement length, simple liquidlike scaling is observed. On the other hand, for $N \gg N_e$, brushlike scaling is found for unconfined films where $d \sim 2R_g$, in agreement with the predic-

tions of Fredrickson *et al.* [15] and confirming the Guiselin brush [16] structure of thin polymer films.

Monodisperse [polydispersity < 1.08] PS films with various thicknesses, ranging from 40 to 2500 Å, and a broad range of molecular weights [MW = (20.8, 45.4, 123, 200, 650, and 900) $\times 10^3$] , were spun cast on to HF etched hydrophobic Si substrates. In order to reach thermal equilibrium [17] and remove residual solvent, the films were annealed well above their glass transition ($T_g \sim 100\,^\circ$C) at 165 °C for over 90 hours in an oil free vacuum of better than 10^{-3} torr. The films were then quenched quickly prior to placement in the x-ray beam. The surface of the films was carefully monitored after annealing and exposure to the x-ray beam, using a Dimension 3000 scanning force microscope where we found no dewetting occurred. The x-ray scattering measurements were performed on Beamline X10B at the Brookhaven National Laboratory (BNL) National Synchrotron Light Source using an energy of 11 keV which corresponds to a wavelength of $\lambda = 1.13$ Å. The scattering experimental geometry is shown as an inset in Fig. 1(a). The scattering vectors, $q_z = (4\pi/\lambda)\sin\alpha_i$ and $q_x = (2\pi/\lambda) \times (\cos\alpha_f - \cos\alpha_i)$, where α_i and α_f, are the incident and exit angles, respectively.

In Fig. 1(a) we show a log-log plot of the diffuse scattering intensity vs q_x for PS (MW = 45.4×10^3) films having thickness, $d = 45$, 67, 187, and 873 Å, at fixed $q_z = 0.233$ Å^{-1}. The van der Waals cutoff ($q_{\rm vdW}$), marked by an arrow, is defined as the locus of the discontinuity in the slope determined by the intersection point between

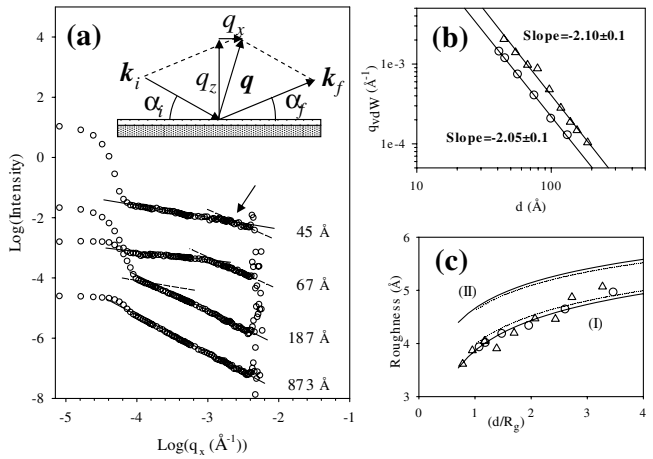

FIG. 1. (a) Diffuse scattering intensity profiles of PS (MW = 45.4×10^3) film are plotted for fixed $q_z = 0.233$ Å^{-1} where $q_{\rm vdW}$ are indicated by arrow. The curves are shifted for clarity. The inset shows the scattering geometry. (b) $q_{\rm vdW}$ are plotted as a function of d for PS 20.8×10^3 (○) and 45.4×10^3 (△). (c) The rms roughness fitted from specular reflectivity are plotted. The fitting lines (MW = 20.8×10^3; dashed and 45.4×10^3; solid line) are calculated from Eq. (1) where the best fit is obtained with $\sigma_{\rm in} = 1$ Å, $q_{\rm vdW}$ obtained from the regression in Fig. 1(b) and $q_{u,c} = 2\pi/\kappa$ with $\kappa = R_g$ (curve I) and $\kappa = a$ (curve II).

parallel dashed and solid lines. From the figure one can see that $q_{\rm vdW}$ moves closer to the specular peak with increasing film thickness, as expected from Eq. (2). Hence for films thicker than $d \sim 200$ Å, only one slope is observed since the $q_{\rm vdW}$'s are now hidden under the specular peak. For $q_x > q_{\rm vdW}$, we find that, as previously observed, the diffuse scattering intensity linearly decreases with q_x and we obtain a constant slope, -1.00 ± 0.05, shown in Fig. 1(a), for the entire range of film thicknesses. For thin films, where the intensity below $q_{\rm vdW}$ can be observed, we find that the intensity is relatively independent of q_x, for all molecular weights studied. For $q_x < q_{\rm vdW}$, we obtain a slope of -0.20 ± 0.03. Hence for low q_x values the liquid films behave like the solid substrate [18].

In Fig. 1(b) we plot the value of $q_{\rm vdW}$ deduced from Fig. 1(a) as a function of film thickness for PS of molecular weight 20.8 and 45.4×10^3 at fixed $q_z = 0.233$ Å^{-1}. The slopes -2.05 ± 0.1 and -2.10 ± 0.1 for PS 20.8×10^3 and for PS 45.4×10^3, respectively, are in good agreement with each other and Eq. (2) confirming the liquidlike behavior of the films. From the intercept and $\gamma_{\rm PS} = 30.3$ dyn/cm at 165 °C we find values of the effective Hamaker constant of $A_{\rm eff} = 2.4 \pm 0.6$ and $11.6 \pm 3.0(\times 10^{-20})$ J for MW = 20.8×10^3 and 45.4×10^3, respectively, which agree within a factor of 2, with the value $A_{\rm eff} = 5.9 \times 10^{-20}$ J obtained by Tidwell *et al.*. From this analysis we can conclude that for molecular weights roughly equal to the entanglement molecular weight, MW $\sim 20 \times 10^3$, the polymer behaves like a simple liquid. On the other hand, the polymeric nature of the films becomes evident when we apply Eq. (1) to fit the surface roughness obtained from the specular reflectivity data as a function of film thickness [Fig. 1(c)]. Here we find that the data all collapse on a single curve when d is scaled with R_g. A good fit to the data for $d < 3R_g$ with Eq. (1) is obtained when we substitute $q_{\rm vdW}$ obtained from the fits in Fig. 1(b) with $\sigma_{\rm in} = 1$ Å and $q_{u,c} = 2\pi/R_g$ [curves (I)]. If we substitute the monomer-monomer distance (a) for κ, as $q_{u,c} = 2\pi/a$, as is commonly done for simple liquids where the shortest wavelength is the intermolecular distance, we obtain large deviations [curves II)] from the experimental data. These results indicate that capillary waves at the surface of very thin films have a liquidlike correlation function [Eq. (1)] except for the fact that the shortest wavelength that can propagate is determined by R_g rather than the monomer-monomer distance. This observation may be due to the fact that R_g is the length scale over which the polymer chains have immobilized segments at the surface, with the number of surface contact points being directly proportional to R_g. As the film thickness increases, fewer chains have surface contacts [19] and the monomer-monomer distance becomes a more appropriate length scale.

Both of the polymer films discussed so far had molecular weights close to the PS entanglement length. In Fig. 2(a) we plot the roughness, obtained from fits to the specular

reflectivity for PS films with $N \gg N_e$ or MW $= 200 \times 10^3$ and 650×10^3 as a function of film thickness. The solid lines are fits to Eq. (1) for the PS film with MW $= 200 \times 10^3$ and 650×10^3 where q_{vdW} is calculated from Eq. (2) using $A_{\mathrm{eff}} = 5.9 \times 10^{-20}$ J, $\sigma_{\mathrm{in}} = 1$ Å, and $q_{u,c} = 2\pi/\kappa$ with $\kappa = R_g$. The dashed line corresponds to Eq. (1) calculated with $\kappa =$ monomer-monomer distance, a. From the figure we find that neither provides a good fit to the data, indicating that it is not possible to fit the higher molecular weight data with the standard liquid capillary wave model, even when the data is scaled with R_g. This can be seen more explicitly when we analyze the diffuse scattering spectra directly. In the inset of Fig. 2(b) we show typical diffuse scattering intensity profiles for a PS (MW $= 650 \times 10^3$) film, 894 Å ($4.1R_g$) thick, plotted as a function of q_x for three different values ofq_z's (0.156, 0.233, and 0.311 Å^{-1}). From the figure we see that the cutoff is independent of q_z, as expected for a liquid film which completely wets a solid substrate. On the other hand, one can see that the curves are parallel to each other which indicates that the slope is also independent of q_z, as previously reported by Wang *et al.* [3]. This is in direct contradiction of simple capillary theory, which predicts intensity, $I \sim q_x^{\eta-1}$ where $\eta = Bq_z^2/2$. Hence high molecular weight polymers do not behave as simple liquids when cast as thin films.

In order to determine the origin of the deviations we then carefully studied the diffuse scattering from films of each molecular weight as a function of film thickness. In Fig. 2(b) we show a typical series of scattering intensity vs q_x profiles for PS (MW $= 650 \times 10^3$) films of different thicknesses at fixed $q_z = 0.233$ Å^{-1}. As in the case of the low molecular weight polymers, the data are fit by two lines whose intersection determines the value of long wavelength cutoff wave vector, $q_{l,c}$ [20]. From the figure we can see that the profiles are qualitatively similar to those obtained from the lower molecular weight films. The slopes on both sides of $q_{l,c}$ appear to be independent of thickness and molecular weight and the values of $q_{l,c}$ shift towards lower values with increasing film thickness as predicted by Eq. (2).

In Fig. 3 we plot $\log(q_{l,c})$ determined from Fig. 2(b) as a function of $\log(d/R_g)$ for various molecular weights [(123, 200, 650, and 900) $\times 10^3$]. The dashed line is drawn to represent $2R_g$ where all chains form Gaussian conformation. From the figure we can see that this is also the line marking a discontinuity in the scaling of $q_{l,c}$ with thickness. For films with $d \gtrsim 2R_g$, $\log(q_{l,c})$ decreases linearly with $\log(d/R_g)$, indicating a uniform power law dependence. The slope varies with molecular weight, in contradiction with Eq. (2) which predicts a constant value of -2, as obtained for MW $= 20.8 \times 10^3$ and 45.4×10^3 (● and ■, respectively).

In the inset of Fig. 3 we plot the slope as a function of R_g, together with the data (PS, MW $= 90 \times 10^3$) from Wang *et al.* [3]. From the figure we see that the slopes are all less than the predicted value of -2 and inversely with R_g. For $d > 3R_g$, we know from Ref. [19] that none of the chains have direct contacts with the surface, yet some-

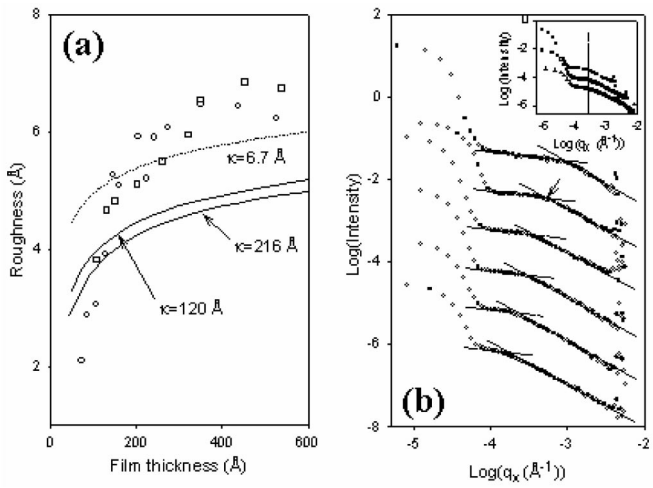

FIG. 2. (a) The rms roughness obtained from specular reflectivity for PS films with MW $= 200 \times 10^3$ (○) and 650×10^3 (□) are plotted vs d. Fitting lines are the fit from Eq. (1) where $\sigma_{\mathrm{in}} = 1$ Å, $A_{\mathrm{eff}} = 5.9 \times 10^{-20}$ J, and $q_{u,c} = 2\pi/\kappa$ with $\kappa = a$ (dashed line) and $\kappa = R_g$ of MW $= 200 \times 10^3$ and 650×10^3 (solid lines). (b) Diffuse scattering intensity of PS (MW $= 650 \times 10^3$) film with $d = 129$, 259, 536, 754, 1176, and 1680 Å from the top are plotted as a function of q_x at fixed $q_z = 0.233$ Å^{-1}. $q_{l,c}$ are indicated by arrows. The curves are shifted for clarity. Inset: Diffuse scattering profiles 894 Å film is plotted at three different q_z of 0.156 (○), 0.233 (□), and 0.311 (△) Å^{-1}. Vertical dashed line indicates $q_{l,c}$.

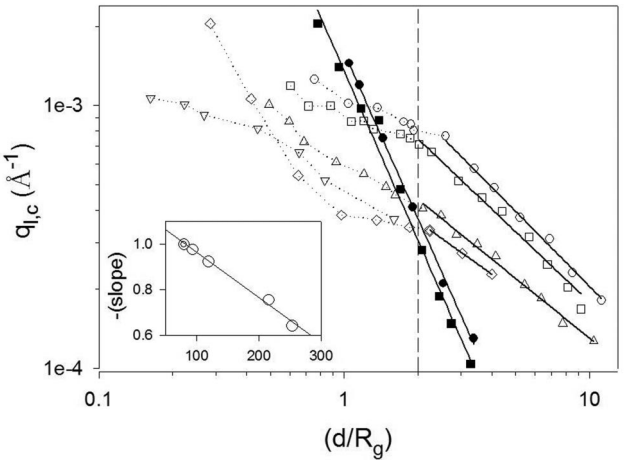

FIG. 3. The values of $q_{l,c}$, as determined from the diffuse scattering measurements, are plotted as a function of (d/R_g) for PS films with MW $=$ [20.8 (●), 45.4 (■), 123 (○), 200 (□), 650 (△), and 900(◇)] $\times 10^3$. Solid lines are linear regression lines and dotted lines are only guidelines. Vertical line indicates $d = 2R_g$. Inset: slopes of the regression lines are plotted as a function of R_g, where data (◎) of PS films with MW $= 90 \times 10^3$ is taken from Ref. [3].

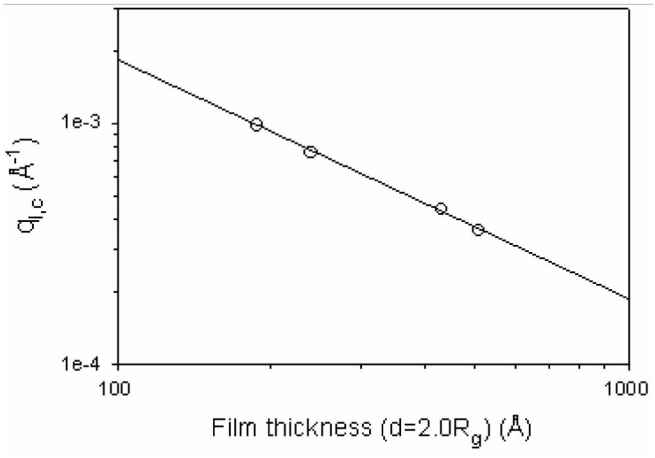

FIG. 4. $q_{l,c}$ with four different MW [(123, 200, 650, and 900) $\times 10^3$] of PS films obtained from regression line in Fig. 3 are plotted as a function of the film thickness at $d = 2R_g$. Solid lines are a linear regression with slope $= -1.1 \pm 0.1$, which is in agreement with the brush model.

how the interfacial interactions seem to propagate to the film surface introducing anomalous surface behavior.

Guiselin *et al.* [16] predicted that when homopolymers adsorb on a surface from the melt, they form a brushlike structure. If the interactions with the surface are attractive, the adsorption is irreversible and several groups have shown that the height of the brush (h_0) scales as the polymerization index of the polymer, $h_0 \sim N^{1/2}$. Fredrickson *et al.* [15] have argued that the surface pinning should be reflected in the capillary spectra of a brush since chain confinement also limits the capillary modes that can propagate to the film surface. Hence, instead of q_{vdW}, they predict that for a grafted brush of grafting density, s, the long wavelength cutoff vector is given by

$$q_{l,c} = (3\mu_0/\gamma)^{1/4} h_0^{-3/4}, \tag{3a}$$

$$\mu_0 = 3k_B T \upsilon s^2/b^2, \tag{3b}$$

where μ_0 is the bulk shear modulus, b is the statistical segment length, and υ is the monomer volume.

If we consider a polymer film adsorbed on a substrate as a Guiselin brush [21], then for an unperturbed film, approximately $2.0R_g$ thick, we can assume that grafting density, s, is calculated from Gaussian chain conformation, $s = N^{1/2}/\pi R_g^2$, and hence $q_{l,c} = \text{constant} \times R_g^{-1.25}$ where $h_0 = 2R_g$.

In order to probe this relationship, we plot $q_{l,c}$ on a log-log scale in Fig. 4 as a function of film thickness, d, where $d = 2.0R_g$ for the particular molecular weight. From the slope of the solid line shown we find that $q_{l,c}$ scales as the brush height raised to a power of -1.1 ± 0.1 which is in good agreement with the predictions of Fredrickson *et al.*. It should be noted that the agreement with the predicted intercept is not as good [22], but this may be due to the fact that the model is not detailed enough to yield an accurate value for the intercept since the equations are derived through a series of scaling relationships based dimensional analysis.

Films that are less than $2R_g$ thick are also composed of polymer chains that contact the surface, but now the chains have more than $N^{1/2}$ contacts with the surface and they are no longer Gaussian. In this case their structure can no longer be described by the Guiselin model. Furthermore, since they are more similar to cross-linked membranes, additional modes may be removed and more extensive analysis is required in order to model the anomalous behavior, observed in Fig. 3, and the effects of increasing confinement on the capillary modes that are allowed to propagate through the film.

We would like to acknowledge the NSF-MRSEC and the NSF Binational programs for support of this work.

[1] K. S. Gautam *et al.*, Phys. Rev. Lett. **85**, 3854 (2000).
[2] R. L. Jones *et al.*, Macromolecules **34**, 559 (2001).
[3] J. Wang *et al.*, Phys. Rev. Lett. **83**, 564 (1999).
[4] R. L. Jones *et al.*, Nature (London) **400**, 146 (1999).
[5] K. Shin *et al.*, Macromolecules **34**, 4993 (2001).
[6] W. Zhao *et al.*, Phys. Rev. Lett. **70**, 1453 (1993).
[7] P. Silberzan *et al.*, Macromolecules **25**, 1267 (1992).
[8] B. Frank *et al.*, Macromolecules **29**, 6531 (1996).
[9] E. K. Lin *et al.*, Macromolecules **32**, 3753 (1999); Z. Li *et al.*, Macromolecules **31**, 1915 (1998); Y. M. Zhang *et al.*, Langmuir **17**, 4437 (2001); X. Zheng *et al.*, Phys. Rev. Lett. **79**, 241 (1997).
[10] O. H. Seeck *et al.*, Europhys. Lett. **29**, 699 (1995).
[11] M. Tolan *et al.*, Physica B (Amsterdam) **221**, 53 (1996).
[12] I. M. Tidswell *et al.*, Phys. Rev. Lett. **66**, 2108 (1991); B. M. Ocko *et al.*, Phys. Rev. Lett. **72**, 242 (1994); M. K. Sanyal *et al.*, Phys. Rev. Lett. **66**, 628 (1991).
[13] K. Shin *et al.*, Macromolecules **34**, 5620 (2001).
[14] Z. Li *et al.*, Macromolecules **31**, 1915 (1998).
[15] G. H. Fredrickson *et al.*, Macromolecules **25**, 2882 (1992).
[16] O. Guiselin, Europhys. Lett. **17**, 225 (1992).
[17] X. S. Hu *et al.*, High Performance Polymers **12**, 621 (2000).
[18] S. K. Sinha *et al.*, Phys. Rev. B **38**, 2297 (1988).
[19] Y. Pu *et al.*, Phys. Rev. Lett. **87**, 206101 (2001).
[20] Since Eq. (1) cannot be used to fit the data for high MW PS, we cannot assume that $q_{l,c}$ is simply determined by the van der Waals cutoff [Eq. (2)].
[21] Reflectivity measurements on end terminated PS (MW $= 102 \times 10^3$) were also carried out and the results were found to be indistinguishable from those on nonterminated films of the same thickness. This is consistent with the findings of Zhao *et al.* [Europhys. Lett. **15**, 725 (1991)].
[22] The intercept in Fig. 4 is 0.175 and the predicted value of the intercept in Eq. (3) is 2.48 where $b = a = 6.7$ Å, $\gamma = 30.3$ dyn/cm, and $\upsilon = 175$ Å^3.